UNIVERSIDAD COMPLUTENSE DE MADRID

FACULTAD DE CIENCIAS FÍSICAS

Máster en Física Teórica

TRABAJO DE FIN DE MÁSTER

Función de fragmentación dependiente de momento transverso de gluon a J/ψ

J/ψ transverse momentum dependent gluon fragmentation function

Samuel Fernández Romera

Directores

Prof. Ignazio Scimemi

Prof. Miguel García Echevarría

Curso académico 2021-22

J/ψ transverse momentum dependent gluon fragmentation function
Master's Thesis

Author
Samuel Fernández Romera
Universidad Complutense de Madrid
Facultad de Ciencias Físicas
samfer04@ucm.es

Tutors
Ignazio Scimemi
Departamento de Física Teórica,
Universidad Complutense de Madrid
ignazios@ucm.es

Miguel G. Echevarría
Departamento de Física,
Universidad del País Vasco
miguel.garciae@ehu.eus
(Dated: June 8, 2022)

One of the relevant mechanisms for the semi-inclusive production of J/ψ at the electron-ion collider is through gluon fragmentation. When the transverse momentum of the J/ψ is measured, the cross-section is given in terms of, among other objects, a gluon transverse-momentum-dependent fragmentation function (TMDFF), which is introduced for the first time here and is the main object of this work. After reviewing the basics of factorization for this kind of processes in soft-collinear effective theory, we present an original perturbative calculation of the gluon TMDFF into J/ψ at next-to-leading order, using non-relativistic QCD. The work reports the progress of this study up to the present date and its future perspectives.

I. INTRODUCTION

The motivation of this work is to contribute to the knowledge of the most fundamental particle physics. In particular, the internal partonic structure of nucleons through the study of quarkonia production.

In quantum chromodynamics (QCD), the charm and bottom are called heavy quarks, and hadrons with heavy quarks are known as heavy hadrons. Quarkonia are bound states composed of a heavy quark and its antiquark. Due to the high scale provided by the large mass of the heavy quarks, heavy hadrons including quarkonia can be used as tools to explore the structure of nucleons and nuclei, the phase diagram of QCD, the spin content of nucleons, the coupling of the Higgs boson to heavy quarks, etc [1, 2]. In general, quarkonia are an important asset for the study of QCD in high-energy collisions.

Over the years, the energy used in the colliders has been increasing, making it possible to study the hadrons more deeply and to observe new properties such as its size, the charge distribution or the confinement of quarks. The deep inelastic scattering experiments allowed to see that by illuminating the proton with a virtual photon with a small wavelength, the proton starts to behave like a free Dirac particle. In other words, the proton is made up of more fundamental particles, and they are called partons. These partons are charged (quarks) and neutral (gluons). In this context, the study of form factors, which define the properties of a certain particle interaction, and parton distribution functions (PDFs), which give the probability of finding partons in a hadron as a function of the longitudinal fraction z of the hadron's momentum carried by the parton, appears. The systems described by the PDFs are not sensitive to the transverse momentum, p_T, of the partons, so with the PDFs we can only obtain a 1D image of the internal structure of the nucleon. However, when the p_T is small compared to the energy of the center of mass of the process, it is required to take into account its contribution in the probability distributions. In this case, the system cannot be described by PDFs and it is necessary to introduce the transverse-momentum-dependent distributions (TMDs). The TMDs are functions of both z and the parton's transverse momentum, and they provide a 3D picture of the internal structure of nucleon. Since they are more fundamental quantities than PDFs and give us more information about non-perturbative QCD, we will study them making use of quarkonia production.

To date, there are many processes of J/ψ production. For example, the proton-proton collision at the a large ion collider experiment (ALICE) [3] or the e^+e^- collision at the BaBar detector [4]. We focus on the future electron-ion collider (EIC). In this experiment processes like $\ell + p \to \ell + J/\psi + X$ or $\ell + p \to \ell + J/\psi + \text{jet} + X$ may occur, where ℓ is any lepton and X stands for the remnants of the collision, an object we do not study. The way in which the internal structure of the proton (quarks and gluons) interacts with the virtual photon, such as $\gamma^* q \to qg$ or $\gamma^* g \to q\bar{q}g$, can give rise to a large number of contributions to the process [5]. The J/ψ production is given by different mechanisms. Among these mechanisms, we focus on gluon fragmentation, described by the TMD fragmentation function (TMDFF). In ref. [6] the TMDFF of light quarks into J/ψ was calculated, a work which is related to this. In addition, to describe these processes it is necessary to use other TMDs such as the TMD parton distribution functions (TMDPDFs). Figure 1 shows two different production mechanisms for J/ψ which contribute to the cross-section: on one side the direct production of quarkonia in photon-gluon fusion through the production of a heavy-quark pair, and on the other the production of J/ψ through gluon fragmentation mechanism.

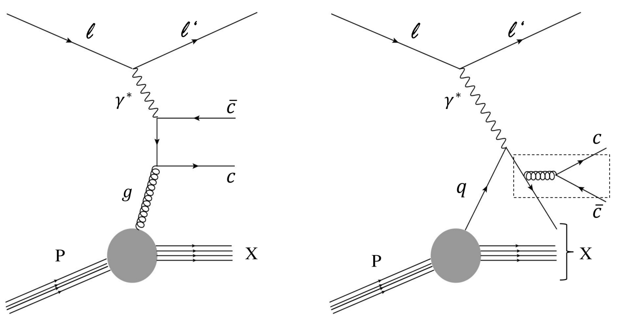

FIG. 1. Two contributions for the process $\ell + p \to \ell + J/\psi + X$. The left picture shows the photon-gluon fusion mechanism and right picture gluon fragmentation mechanism. The rectangle in the right picture indicates the TMDFF we have computed in this work.

The processes we are describing are of high-energy physics. In these experiments the hadrons come from collimated jets with much less energetic particles and it is common to use soft-collinear effective theory (SCET) [7, 8]. In this effective theory there are different regions of momentum in which the degrees of freedom of the system can be defined. The momentum components of the particles are usually described by a scaling parameter $\lambda \ll 1$, which for our case is defined as $\lambda = p_\perp/M$ [9], where $p_\perp$ is the transverse momentum component of the J/ψ and the jet, if any, and M is the mass of the J/ψ or the invariant mass of the J/ψ+jet. The most important result of this effective theory is that it allows us to factorize the cross section of any process based on the energy scale [10]. Thus, we are able to calculate each part independently with different models and techniques.

Nonrelativistic QCD (NRQCD) is another effective theory that we need to describe the heavy quarkonium in the final state [11]. NQRCD is based on the idea that heavy quarks are non-relativistic and we can consider that their velocity is $v \ll 1$. Analogous to SCET, with NRQCD we can factorize the quantities of interest in different energy regions where in this case the scaling parameter is v. In particular, this argument allows us to decompose the TMDFF in terms of calculable short-distance coefficients, which describe the production of heavy-quarks pair in a particular angular momentum, and long-distance matrix elements (LDMEs), which describe the decay of the heavy-quarks pair into the final color quarkonium state. The short-distance coefficients is the one we are going to calculate in this work, where all the dynamics of the process is hidden.

The LDMEs are described by the color and angular momentum configuration in which the quark-antiquark pair is found and which is denoted as $n = {}^{2S+1}L_J^{[col.]}$ with parity $P = (-1)^{L+1}$ and charge conjugation number $C = (-1)^{L+S}$ in a color singlet state. Therefore the quark-antiquark pair must be in a color single state and in a configuration that is consistent with the quantum numbers J^{PC} of the meson. Those states are suppressed by others with different configuration due to the expansion in v, and the scenario is different for different final states. For our case, J/ψ has the quantum numbers $J^{PC} = 1^{--}$, so we need a configuration with $J = 1$ and $L + S$ an odd number. By using the v expansion we obtain ${}^3S_1^{[1]} \sim v^3$, ${}^3S_1^{[8]} \sim v^7$, ${}^1S_0^{[8]} \sim v^7$ and ${}^3P_J^{[8]} \sim v^7$ for J/ψ production [11].

In summary, we need SCET to describe the energetic hadrons and soft radiation of the initial state, and we need NRQCD for the heavy quarkonium in the final state. Each of these theories is described by a small parameter, λ for SCET and v for NRQCD. The way these parameters are related describes different scenarios. For example we can consider $v \sim \lambda$, where the soft regions of both theories overlap and have the same soft gluons, or $v \ll \lambda$ where it is necessary to work with both theories.

The objective of this work is to calculate the virtual gluon contribution to the TMDFF at next-to-leading order, and use it to check that the structure of divergences agrees with TMD factorization. The work is organized as follows: in sec. II we discuss relevant aspects of SCET and the conventions used in the calculation. In sec. III we show the expression of the gluon TMDFF. In sec. IV we discuss the matching of the TMDFF with the NRQCD. Finally, in the remaining sections we show the calculation necessary to arrive at the result.

II. LIGHT-CONE COORDINATES

It is convenient to use light-cone coordinates to describe jets of energetic hadrons in SCET. We choose a light-cone vector $n^\mu = (1, 0, 0, 1)$ in the direction of the one of the energetic jets and its complementary $\bar{n}^\mu = (1, 0, 0, -1)$ such that $n \cdot \bar{n} = 2$ and $n^2 = \bar{n}^2 = 0$. With this vectors we can represent any four-vector as

$$p^+ = n \cdot p, \quad p^- = \bar{n} \cdot p, \tag{1}$$

$$p^\mu = p^+ \frac{\bar{n}^\mu}{2} + p^- \frac{n^\mu}{2} + p_\perp^\mu, \tag{2}$$

$$p^2 = p^+ p^- + p_\perp^2 = p^+ p^- - p_T^2. \tag{3}$$

The components of the momentum, $p^\mu = (p^+, p^-, p_\perp)$, can be parameterized with λ parameter such that we can distinguish the different kinematical regions. The scaling of the relevant degrees of freedom (d.o.f.) are $p_n^\mu \sim Q(\lambda^2, 1, \lambda)$ and $p_s^\mu \sim Q(\lambda^2, \lambda^2, \lambda^2)$, where Q is the typical hard scale. The power counting of collinear d.o.f. correspond to $p^2 \sim \lambda^2 Q^2$ that is boosted in the n-direction. For soft d.o.f the power counting correspond to $p^2 \sim \lambda^4 Q^2$, describing much less energetic radiation without a preferred direction.

III. TMD FRAGMENTATION FUNCTION

As mentioned in the introduction, SCET allows factoring the cross section of the process. The most interesting factors are the TMDs because they represent a crucial step in the understanding of ordinary matter. The other factors that appear as a result of the factorization can be calculated perturbatively and are related to the hard part of the process.

In gluon fragmentation the TMD involved is the TMDFF. It is represented graphically inside the rectangle in the right picture of Fig. 1 and is defined by the equation (4) [12], which shows the unsubtracted hadronic matrix elements of the TMDFF operators,

$$\begin{aligned}&\Delta_{g\to J/\psi}(z,\mathbf{b}_\perp)\\ &= \frac{-1}{2(1-\epsilon)P^+(N_c^2-1)}\sum_X \int \frac{d\xi^-}{2\pi} e^{-iP^+\xi^-/z}\\ &\times \langle 0|T\left[\mathcal{B}^\mu_{n\perp}\right]\left(\frac{\xi}{2}\right)|X, J/\psi\rangle\langle X, J/\psi|\bar{T}\left[\mathcal{B}_{n\perp\mu}\right]\left(\frac{-\xi}{2}\right)|0\rangle\,,\end{aligned} \tag{4}$$

where the variable z is the momentum fraction of the parton inside the hadron and $\mathbf{b}_\perp$ is the conjugate variable of transverse momentum. The prefactor is a normalization constant related with color and polarizations in $d = 4-2\epsilon$ dimension, $\xi = \{0^+, \xi^-, \mathbf{b}_\perp\}$ and $\mathcal{B}^\mu_{n\perp}$ is the gluon field strength defined as

$$\mathcal{B}^\mu_{n\perp} = \frac{1}{g}[W_n^\dagger(y) i D^\mu_{n\perp} W_n(y)], \tag{5}$$

with $iD^\mu_{n\perp} = \mathcal{P}^\mu_{n\perp} + gA^\mu_{n\perp}$, the label momentum operator and the composite SCET field of n-collinear gluons respectively. In (5), W_n are the collinear Wilson lines defined in the following way

$$W_n(y) = P\exp\left[ig\int_{-\infty}^0 ds\bar{n}\cdot A_n^a(y+\bar{n}s)t^a\right], \tag{6}$$

where P indicate path-ordered, $A^a(x)$ is the gluon field and t^a are the $SU(N_c)$ generators.

In order to renormalize the TMDFF, it should be noted that in SCET there are divergences that are neither ultraviolet (UV) nor infrared (IR), they are known rapidity divergences. This kind of divergences arise when the plus or minus component of the loop momentum is boosted to infinity in one light-cone direction, that is for example $k^+ \to \infty$ such that the product k^+k^- is fixed. Thus, in order to remove UV and rapidity divergences we define the renormalized TMDFF as follows

$$D_{g\to J/\psi}(z,\mathbf{b}_\perp,\mu,\zeta) = Z_g(\zeta,\mu)R_g(\zeta,\mu)\Delta_{g\to J/\psi}(z,\mathbf{b}_\perp)\,, \tag{7}$$

where Z_g is the usual renormalization factor for UV divergences and R_g is the rapidity renormalization factor, μ is the scale of UV subtraction and ζ is the scale of rapidity subtraction. Here, R_g is defined as follows

$$R_g(\zeta,\mu) = \frac{\sqrt{S(\mathbf{b}_\perp)}}{\mathbf{Z_b}}, \tag{8}$$

which includes the soft overlap contribution through the term $\mathbf{Z_b}$ [13], and the soft function denoted as $S(\mathbf{b}_\perp)$. The soft function (SF) [14] is defined as a expectation value of Wilson lines:

$$S(\mathbf{b}_\perp) = \frac{\mathrm{Tr}_c}{N_c^2-1}\langle 0|T[S_n^\dagger \tilde{S}_{\bar{n}}](0^+,0^-,\mathbf{b}_\perp)\bar{T}[\tilde{S}_{\bar{n}}^\dagger S_n](0)|0\rangle\,, \tag{9}$$

where $S_n = P\exp\left[ig\int_{-\infty}^0 dsn\cdot A_s(x+ns)\right]$ are the soft Wilson lines.

In addition to calculating the gluon TMDFF, we want to check that the factor renormalization (8) effectively eliminates all rapidity divergences in the case of quarkonia production by gluon fragmentation.

IV. TMDFF REFACTORIZATION

The factorization in quarkonia production resides in the idea of separating the relativistic physics of the heavy-quarks production from the non-relativistic physics of quarkonia structure, and NRQCD is an effective theory which allows us to achieve it.

We employ NRQCD factorization formalism [15] to write the TMDFF as a product of matching coefficients and matrix elements:

$$D_{g\to J/\psi}(z,\mathbf{b}_\perp) = \sum_{mn} d_{mn}(z,\mathbf{b}_\perp)\langle\mathcal{O}_{mn}^{J/\psi}\rangle\,, \tag{10}$$

where $d_{mn}(z,\mathbf{b}_\perp)$ are the short-distance coefficients. All relativistic effects are absorbed in these coefficients which can be calculated as a perturbative series in the strong coupling constant, α_s. The matrix elements $\langle\mathcal{O}_{mn}^{J/\psi}\rangle$ are the so-called long-distance matrix elements (LDMEs) of NRQCD, defined as follows:

$$\langle\mathcal{O}_{mn}^{J/\psi}\rangle = \langle 0|\chi^\dagger\mathcal{K}_m\psi a^\dagger_{J/\psi}a_{J/\psi}\psi^\dagger\mathcal{K}'_n\chi|0\rangle\,, \tag{11}$$

where $a_{J/\psi}$ and $a^\dagger_{J/\psi}$ are the operators of annihilation and creation of the state describing the J/ψ, $\mathcal{K}_n$ and $\mathcal{K}'_n$ are products of a color matrix, a spin matrix and other fields, and χ and ψ are the field operators for the heavy quarks in NRQCD.

The short-distance coefficients in (10) can be obtained by matching the perturbative calculation of the TMDFF in which the J/ψ is replaced by a $c\bar{c}$ pair. This state is characterized by a total momentum P, a relative spatial momenta $\mathbf{q}$ in the $c\bar{c}$ rest frame, that in the threshold $\mathbf{q}=0$, and by the spin and color specified by the spinors of the heavy quarks. Then, the first step to find d_{mn} is to calculate the left-hand side of the equation (10) around the threshold. This is equivalent to computing the TMDFF (7) by substituting the J/ψ projector for the $c\bar{c}$ projector described above:

$$\mathcal{P}_{J/\psi} = \sum_X |X, J/\psi(P)\rangle \langle X, J/\psi(P)| \\ \longrightarrow \sum_X |X, c(p,\xi)\bar{c}(p',\eta)\rangle \langle X, c(p,\xi)\bar{c}(p',\eta)| , \qquad (12)$$

where ξ and η are the spinors of the heavy quarks, and p and p' their momentums, which satisfy $p+p'=P$. The second step is to compute the right-hand side of equation (10) using perturbative NRQCD and expanding in powers of $\mathbf{q}$. Finally, we obtain the short-distance coefficients by matching the expansions in $\mathbf{q}$, order by order in α_s, of the two sides of (10).

V. SHORT-DISTANCE COEFFICIENTS COMPUTATION

The type of diagrams we need to calculate are shown in figures 2 y 3, which were obtained by expanding the matrix elements in (4) at different orders of g. In this work we have only computed the LO diagram and NLO virtual diagrams contributions.

We use the SCET Feynman rules from ref. [14] for the gluon field strength, $\mathcal{B}^\mu_{n\perp}$, defined in (5):

$$\mathcal{B}^{\mu\alpha,ca}_{n\perp} = \delta^{ca}\left(g^{\mu\alpha}_\perp - \frac{p^\mu_\perp \bar{n}^\alpha}{\bar{n}\cdot p}\right), \qquad (13)$$

$$\mathcal{B}^{\mu\alpha\beta,cab}_{n\perp} = igf^{cab}\left[\frac{g^{\mu\beta}_\perp}{\bar{n}\cdot p} - \frac{g^{\mu\beta}_\perp \bar{n}^\alpha}{\bar{n}\cdot q} \right. \\ \left. + \left(\frac{p^\mu_\perp}{\bar{n}\cdot q} - \frac{q^\mu_\perp}{\bar{n}\cdot p}\frac{\bar{n}^\alpha\bar{n}^\beta}{\bar{n}\cdot(q+p)}\right)\right], \qquad (14)$$

where (13) is the SCET Feyman rule at order $\mathcal{O}(g^0)$ of $\mathcal{B}^\mu_{n\perp}$ and (14) at order $\mathcal{O}(g)$.

To regulate rapidity divergences we use δ-regulator [16]. This implementation is done at the level of the operators by modifying the Wilson lines as follows

$$W_n(y) = P\exp\left[ig\int_{-\infty}^0 ds\,\bar{n}\cdot A^a_n(x+\bar{n}s)t^a\right] \\ \longrightarrow P\exp\left[ig\int_{-\infty}^0 ds\,\bar{n}\cdot A^a_n(x+\bar{n}s)t^a e^{\delta^- s}\right], \qquad (15)$$

where the difference with (6) is in the exponential of the δ-regulator. The only diagrams in which we have to use this regularization scheme are Fig. 3(c,d,e).

For the calculation we are going to divide the contribution of each Feynman diagram into a leptonic part and a gluonic part. The gluon tensor will be constructed by combining the SCET Feynman rules of $\mathcal{B}^\mu_{n\perp}$ with the QCD Feynman rules, corresponding to the gluons linking the heavy-quarks vertices with the eikonal lines. For the fermionic part we will use the Feynman rules of QCD.

A. Leading Order

In this case (Fig. 2), the gluon tensor is constructed by two gluon propagators of QCD and two Feynman rules (13), one for each side of the cut diagram:

$$G^{ab,LO}_{\alpha\beta} = \delta^{ab}\frac{i^2}{(P^2)^2}\left(g_{\alpha\beta} - \frac{P_\alpha\bar{n}_\beta + P_\beta\bar{n}_\alpha}{\bar{n}\cdot P} + \frac{\bar{n}^\alpha\bar{n}^\beta P^2}{(\bar{n}\cdot P)^2}\right), \qquad (16)$$

where P is the total momentum $P^2 = 4E_c^2$ with $E_c = \sqrt{m_c^2+\mathbf{q}^2}$ and $\mathbf{q}$ is the relative momentum in the center of momentum frame of the heavy quarks.

The fermionic tensor is made by two quark-gluon vertices of QCD, one of each side of the cut diagram:

$$L^{ab,LO}_{\alpha\beta} = [\bar{u}(p)(ig\gamma_\alpha T^a)v(p')][\bar{v}(p')(ig\gamma_\beta T^b)u(p)], \qquad (17)$$

where p and p' are the momentums of the heavy quarks. At this point, we carry out the spinorial expansion around the threshold, $\mathbf{q}=0$, summarized in the formulas found in the appendix A of ref. [17]. Thus,

$$\bar{u}(p)\gamma^\mu v(p') \simeq 2m_c L^\mu_j \xi^\dagger\sigma^j\eta, \qquad (18)$$

where ξ and η are the Pauli spinors, σ's are the Pauli matrices and L is the Lorentz boost from the heavy quarkonium center of mass frame to the boosted collinear frame, which satisfies the following properties

$$-g_{\alpha\beta}L^\alpha_i L^\beta_j = \delta^{ij}, \quad L^\alpha_i L^\beta_i = -g^{\alpha\beta} + \frac{P^\alpha P^\beta}{P^2}, \\ \bar{n}^\alpha L_{\alpha,i} = \frac{\bar{n}\cdot P}{\sqrt{P^2}}\hat{z}^i. \qquad (19)$$

Therefore,

$$L^{ab,LO}_{\alpha\beta} = -g^2(2m_c)^2 L^\alpha_i L^\beta_j[\xi^\dagger\sigma^i T^a\eta\eta^\dagger\sigma^j T^b\xi]. \qquad (20)$$

For the unpolarized case we sum over all polarizations, so we need to normalize with the total number of polarizations, being $D-1$ in a D-dimensional spacetime,

$$L^{ab,LO}_{\alpha\beta} = -\frac{g^2(2m_c)^2}{D-2} L^\alpha_i L^\beta_j \sum_{pol.} [\xi^\dagger \sigma^i T^a \eta\eta^\dagger \sigma^j T^b \xi]$$
$$= -\frac{g^2(2m_c)^2}{D-2} L^\alpha_i L^\beta_j \delta^{ij} [\xi^\dagger \sigma^k T^a \eta\eta^\dagger \sigma^k T^b \xi]. \quad (21)$$

The result of contracting (21) with (16) forms the matrix element of the left-hand side of equation (10), or equivalently the matrix element of equation (4). Now we have to do the matching with the right hand side. From ref. [11] the spinorial factor of (21), in square brackets, corresponds to the expansion at LO in α_s of the NRQCD matrix element:

$$\langle \chi^\dagger \sigma^k T^a \psi \mathcal{P}_{J/\psi} \psi^\dagger \sigma^k T^b \chi \rangle \mid_{pNRQCD}$$
$$\approx 4m_c^2 (D-1)[\xi^\dagger \sigma^k T^a \eta\eta^\dagger \sigma^k T^b \xi], \quad (22)$$

so the tensor (21), as a function of LDMEs, is described by

$$L^{ab,LO}_{\alpha\beta} = -\frac{g^2(2m_c)^2}{(D-2)(D-1)(2m_c)^2} L^\alpha_i L^\beta_i$$
$$\times \langle \chi^\dagger \sigma^k T^a \psi \mathcal{P}_{J/\psi} \psi^\dagger \sigma^k T^b \chi \rangle . \quad (23)$$

If we contract (23) with (16) and introduce the result in (4) we obtain the short-distance coefficient at LO:

$$d^{LO}(z, \mathbf{b}_\perp) = \frac{\pi \alpha_s \mu^{2\epsilon}}{8 m_c^3 (D-1)} \delta(1-z) \delta^{(2)}(\mathbf{b}_\perp), \quad (24)$$

where the $1/8$ comes from averaging over the color states, $N_c^2 - 1 = 8$ for gluons. The $D-2$ factor of (23) has canceled with the $D-2$ factor that comes from contracting (16) with (23). Also, in (24) there is a additional factor $1/4m_c$ of the operator in NRQCD. The Dirac deltas come from the exponential of the TMDFF definition. The term $\delta(1-z)$ reflects the fact that the J/ψ takes away all the momentum of the fragmenting gluon.

To conclude the discussion we can study in depth the transverse and longitudinal behavior denoting $\hat{z}^i$ as the unitary fraction gluon energy vector. If we recalculate the contraction of the gluon tensor and the fermionic tensor using the relations of (19), we find a purely transverse behavior

$$\sim (\delta^{ij} - \hat{z}^i \hat{z}^j) \xi^\dagger \sigma^j T^a \eta\eta^\dagger \sigma^i T^a \xi, \quad (25)$$

and as we will see soon, the virtual contribution at NLO has the same behaviour. Only in real gluon diagrams we obtain a longitudinal contribution, but this is not shown in this work.

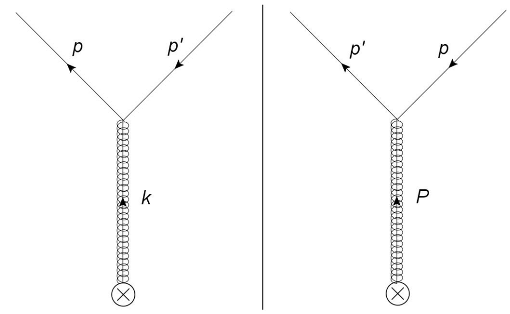

FIG. 2. Diagram contributing to LO. The circles with crosses inside them with an outgoing collinear gluon are the graphical representation of (13). At LO, $k = P$.

B. Next-to-leading order diagram c

In this case (Fig. 3,c) we need to use (14) and a QCD gluon propagator,

$$\sim \left(\frac{i\delta^{ab} g_{\alpha\beta}}{q^2}\right) \left[igf^{cab} \left(\frac{g_\perp^{\mu\beta} \bar{n}^\alpha}{\bar{n}\cdot k} - \frac{g_\perp^{\mu\alpha} \bar{n}^\beta}{\bar{n}\cdot q} + \left(\frac{p_\perp^\mu}{\bar{n}\cdot q} - \frac{q_\perp^\mu}{\bar{n}\cdot p} \right) \frac{\bar{n}^\alpha \bar{n}^\beta}{\bar{n}\cdot(p+q)} \right) \right], \quad (26)$$

but with the properties of the reference vectors indicated in sec. II, $\bar{n}^\alpha g_{\perp,\alpha\beta} = 0, \bar{n}^2 = 0$, we obtain that it is zero.

C. Next-to-leading order diagram d

In this case (Fig. 3,d), we have a more difficult structure for gluon tensor and fermionic tensor because there are two ways to connect the gluons from eikonal line with quark-gluon vertices. The only difference between both is the index interchange between γ's in the quark-gluon vertex and the momentum interchange in the SCET Feynman rule (14). Also we have to swap the color indexes of the group elements. Therefore, the gluon tensors for the two subcases are

$$G^{abc,d1}_{\alpha\beta\sigma} = \frac{i^3 g f^{bac}}{P^2 (k^2 + i\epsilon)((k-P)^2 + i\epsilon)} \frac{1}{\bar{n}\cdot(k-P)}$$
$$\times \left[\bar{n}^\sigma g^{\alpha\beta} \left(1 - \frac{\bar{n}\cdot P}{\bar{n}\cdot k}\right) + \bar{n}^\alpha g^{\beta\sigma} - \frac{k^\beta \bar{n}^\alpha \bar{n}^\sigma}{\bar{n}\cdot k} + \bar{n}^\beta \bar{n}^\sigma P^\alpha \right.$$
$$\times \left(\frac{1}{\bar{n}\cdot k} - \frac{1}{\bar{n}\cdot P} \right) + \bar{n}^\alpha \bar{n}^\sigma P^\beta \left(\frac{1}{\bar{n}\cdot k} - \frac{1}{\bar{n}\cdot P} \right) - \frac{\bar{n}^\alpha \bar{n}^\beta P^\sigma}{\bar{n}\cdot P}$$
$$\left. + \bar{n}^\alpha \bar{n}^\beta \bar{n}^\sigma \left(\frac{k\cdot P}{(\bar{n}\cdot k)(\bar{n}\cdot P)} + \frac{P^2}{(\bar{n}\cdot P)^2} - \frac{P^2}{(\bar{n}\cdot k)(\bar{n}\cdot P)} \right) \right], \quad (27)$$

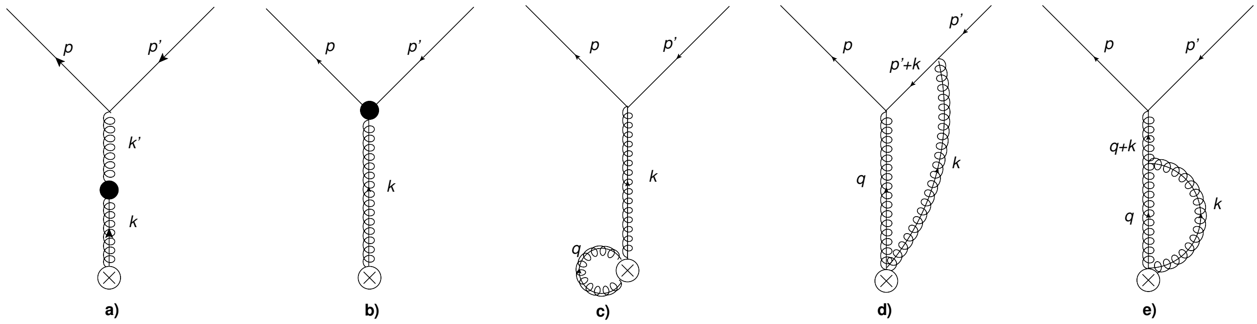

FIG. 3. Virtual diagrams contributing to NLO. We only show one side of the cut diagram. The circles with crosses inside them with two outgoing collinear gluons are the graphical representation of (14). Diagram a) is the correction to gluon propagator and diagram b) is the correction to quark-gluon vertex. The diagram c) or tadpole diagram is zero because there is a gluon loop attached to the eikonal line. Diagram d) also represents the diagram for which we interchange the vertices to which the gluones of diagram d) are connected. Also, we need to take the Hermitian conjugate of every diagram.

and

$$\begin{aligned}G^{abc,d2}_{\alpha\beta\sigma} &= \frac{i^3 g f^{bca}}{P^2(k^2+i\epsilon)((k-P)^2+i\epsilon)}\frac{1}{\bar{n}\cdot(k-P)}\\ &\times\left[-\bar{n}^\sigma g^{\alpha\beta}+\bar{n}^\alpha g^{\beta\sigma}\left(-1+\frac{\bar{n}\cdot P}{\bar{n}\cdot k}\right)+\frac{k^\beta\bar{n}^\alpha\bar{n}^\sigma}{\bar{n}\cdot k}\right.\\ &+\frac{\bar{n}^\beta\bar{n}^\sigma P^\alpha}{\bar{n}\cdot P}+\bar{n}^\alpha\bar{n}^\sigma P^\beta\left(\frac{1}{\bar{n}\cdot P}-\frac{1}{\bar{n}\cdot k}\right)\\ &-\bar{n}^\alpha\bar{n}^\beta P^\sigma\left(\frac{1}{\bar{n}\cdot P}-\frac{1}{\bar{n}\cdot k}\right)\\ &\left.+\bar{n}^\alpha\bar{n}^\beta\bar{n}^\sigma\left(-\frac{k\cdot P}{(\bar{n}\cdot k)(\bar{n}\cdot P)}-\frac{P^2}{(\bar{n}\cdot P)^2}+\frac{P^2}{(\bar{n}\cdot k)(\bar{n}\cdot P)}\right)\right]\end{aligned} \tag{28}$$

On other hand, the fermionic tensors are

$$\begin{aligned}L^{abc,d1}_{\alpha\beta\sigma} &= [\bar{u}(p)(ig\gamma_\alpha T^a)\left(\frac{i(p'+k+m_c)}{(p'+k)^2-m_c^2}\right)\\ &\times(ig\gamma_\sigma T^c)v(p')][\bar{v}(p')(ig\gamma_\beta T^b)u(p)],\end{aligned} \tag{29}$$

and

$$\begin{aligned}L^{abc,d2}_{\alpha\beta\sigma} &= [\bar{u}(p)(ig\gamma_\sigma T^a)\left(\frac{i(p'+k+m_c)}{(p'+k)^2-m_c^2}\right)\\ &\times(ig\gamma_\alpha T^c)v(p')][\bar{v}(p')(ig\gamma_\beta T^b)u(p)].\end{aligned} \tag{30}$$

We will treat the fermionic tensor as in the LO calculation. We are only going to indicate which are the steps for one of them, for example for d1, because for the other one it is the same with the color indices exchanged. We use the following formulas, from appendix A of ref. [17],

$$\bar{u}(p)v(p') \simeq 0, \tag{31}$$

$$\bar{u}(p)(\gamma_\mu\gamma_\nu-\gamma_\nu\gamma_\mu)v(p') \simeq 2(P^\mu L_j^\nu - P^\nu L_j^\mu)\xi^\dagger\sigma^j\eta, \tag{32}$$

$$\begin{aligned}&\bar{u}(p)(\gamma_\mu\gamma_\nu\gamma_\lambda-\gamma_\lambda\gamma_\nu\gamma_\mu)v(p') \simeq\\ &-m_c L_i^\mu L_j^\nu L_k^\lambda \xi^\dagger\{[\sigma^i,\sigma^j],\sigma^k\}\eta.\end{aligned} \tag{33}$$

When we insert these formulas into the fermionic tensor and sum over all polarizations the terms equivalent to (33) cancel out because $\{[\sigma^i,\sigma^j],\sigma^k\} = i4\epsilon^{ijk}$ is antisymmetric. Thus, the fermionic tensor for d1 after sum over all polarizations is

$$\begin{aligned}L^{abc,(d1)}_{\alpha\beta\sigma} &= \frac{i^4 g^3}{(D-2)((p'+k)^2-m_c^2)}\left[(p'+k)^\mu(2m_c)^2\right.\\ &\times\left(g_{\sigma\alpha}L_i^\mu - g_{\sigma\mu}L_i^\alpha - g_{\mu\alpha}L_i^\sigma\right)L_j^\beta + 2m_c^2(P^\alpha L_i^\sigma\\ &\left.-P^\sigma L_i^\alpha)L_j^\beta\right]\delta^{ij}[\xi^\dagger T^a\sigma^i T^c\eta\eta^\dagger\sigma^i T^b\xi].\end{aligned} \tag{34}$$

In this case it is not obvious that we recover the same LDME as in (23) because we have three matrices T's in the spinorial bracket. If we analyze the total color we factor find

$$(f^{bca}T^aT^c)T^b = -i\frac{C_A}{2}T^bT^b, \tag{35}$$

with $C_A = 3$ for SU(3), so this configuration results in the same LDME as LO, described in (23). Note the color factor of d2 introduces a global minus with respect to d1.

Finally we obtain the following result

$$\begin{aligned}d^d(z,\mathbf{b}_\perp) &= d^{d1}(z,\mathbf{b}_\perp) - d^{d2}(z,\mathbf{b}_\perp)\\ &= -d^{LO}(z,\mathbf{b}_\perp)\pi\alpha_s 32 C_A m_c^2\\ \times\mathrm{Im}&\int\frac{d^Dk}{(2\pi)^D}\frac{\bar{n}\cdot k}{k^2\bar{n}\cdot(k-P)(k-P)^2((P/2+k)^2-m_c^2)},\end{aligned} \tag{36}$$

where we have used that $p' = P/2$ for the limit $\mathbf{q} \simeq 0$, Im stands for the imaginary part and we have omitted the $+i\epsilon$ factor in the denominators for simplicity of the notation. If we manipulate this integral, we recover the integrals of sec. VIII. That is,

$$I = \int d^Dk\frac{\bar{n}\cdot k}{k^2(k-P)^2[(k-P/2)^2-m_c^2]\bar{n}\cdot(k-P)}, \tag{37}$$

we can do the shift $k \to k + P$ in the loop momentum k,

$$\begin{aligned} I &= \int d^D k \frac{\bar{n}\cdot(k+P)}{(k+P)^2 k^2[(k+P/2)^2 - m_c^2]\bar{n}\cdot k} \\ &= \int d^D k \frac{1}{(k+P)^2 k^2[(k+P/2)^2 - m_c^2]} \\ &+ \int d^D k \frac{\bar{n}\cdot P}{(k+P)^2 k^2[(k+P/2)^2 - m_c^2]\bar{n}\cdot k}. \end{aligned} \tag{38}$$

The first integral of r.h.s correspond with I_{ABD} doing $P \to -P$ and the second is equal to $\bar{n}\cdot P I_{ABCD}$ after doing $k \to k - P$. Theredore,

$$\begin{aligned} d^d(z, \mathbf{b}_\perp) = &-d^{LO}(z, \mathbf{b}_\perp)\pi\alpha_s 32 C_A m_c^2 \\ &\times(\bar{n}\cdot P I_{ABCD} - I_{ABD}), \end{aligned} \tag{39}$$

where I_{ABCD} y I_{ABD} are the integrals computed in section VIII.

D. Next-to-leading order diagram e

In this case (Fig. 3,e), we need the SCET Feynman rules (13) and (14), a triple gluon vertex of QCD and for gluon propagators of QCD. The result of contracting these feynman rules is as follows

$$\begin{aligned} G^{ab,e}_{\alpha\beta} &= \frac{i^4 g^2 f^{bt_1t_2} f^{t_1t_2a}}{(k^2+i\epsilon)((k-P)^2+i\epsilon)(P^2)^2}\frac{2}{(\bar{n}\cdot(k-P)+i\epsilon)} \\ &\times\left[-g_{\alpha\beta}\left(\bar{n}\cdot(k-P) + \frac{(\bar{n}\cdot P)^2}{\bar{n}\cdot k}\right) + \bar{n}^\alpha P^\beta\left(-1 + \frac{\bar{n}\cdot P}{\bar{n}\cdot k}\right.\right. \\ &\left. + \frac{\bar{n}\cdot k}{\bar{n}\cdot P}\right) + \bar{n}^\beta P^\alpha\left(-1 + \frac{\bar{n}\cdot P}{\bar{n}\cdot k} + \frac{\bar{n}\cdot k}{\bar{n}\cdot P}\right) \\ &\left. + P^2\bar{n}^\alpha\bar{n}^\beta\left(\frac{1}{\bar{n}\cdot P} - \frac{\bar{n}\cdot k}{(\bar{n}\cdot P)^2} - \frac{1}{\bar{n}\cdot k}\right)\right]. \end{aligned} \tag{40}$$

The fermionic tensor is the same as at LO,

$$L^{ab,e}_{\alpha\beta} = -\frac{g^2}{(D-2)(D-1)} L_i^\alpha L_i^\beta \langle\chi^\dagger\sigma^k T^a\psi\mathcal{P}_{J/\psi}\psi^\dagger\sigma^k T^b\chi\rangle \tag{41}$$

We contract (40) with (41) and conclude that the short-distance coefficient is

$$\begin{aligned} d^e(z, \mathbf{b}_\perp) = &-d^{LO}(z, \mathbf{b}_\perp)\pi\alpha_s 8 C_A \,\mathrm{Im}\int\frac{d^D k}{(2\pi)^D}\frac{1}{k^2(k-P)^2} \\ &\times\left[1 + \bar{n}\cdot P\left(\frac{1}{\bar{n}\cdot k - \bar{n}\cdot P} - \frac{1}{\bar{n}\cdot k}\right)\right]. \end{aligned} \tag{42}$$

We recover the I_{AB} integral for the first term within the bracket. We can reexpress the third term doing the sift $k \to k + P$ such that

$$I_3 = \bar{n}\cdot P\int\frac{d^D k}{(2\pi)^D}\frac{1}{(k+P)^2 k^2[\bar{n}\cdot(k+P)]}. \tag{43}$$

This integral is equal to the integral corresponding to the second addend of the bracketed term in equation (42) doing $P \to -P$, but it is odd under this interchange, so the two integrals are added together and the result is

$$d^e(z, \mathbf{b}_\perp) = -d^{LO}(z, \mathbf{b}_\perp) 8\pi\alpha_s C_A(2\bar{n}\cdot P I_{ABC} - I_{AB}), \tag{44}$$

where I_{ABC} y I_{AB} are the integrals in sec. VIII.

VI. FINAL RESULT

After substituting the value of the integrals performed in sec. VIII in the results found in sec. V we conclude that the virtual contribution for the short-distance coefficients at NLO, with the $\overline{\text{MS}}$-scheme ($\mu^2 \to \mu^2 e^{\gamma_E}/(4\pi)$), are

$$\begin{aligned} d^d(z, \mathbf{b}_\perp) &= -d^{LO}(z, \mathbf{b}_\perp)\frac{\alpha_s C_A}{\pi} \\ &\times\left[-\frac{3}{2}\ln^2\frac{\delta^+}{P^+} + 2\ln^2 2 - 2\ln 2 + \frac{19\pi^2}{24}\right], \end{aligned} \tag{45}$$

and

$$\begin{aligned} d^e(z, \mathbf{b}_\perp) = &-d^{LO}(z, \mathbf{b}_\perp)\frac{\alpha_s C_A}{\pi}\left[-\frac{1}{2\epsilon}\left(1 + \ln\frac{\delta^{+2}}{P^{+2}}\right)\right. \\ &+ \frac{1}{2}\ln^2\frac{\delta^+}{P^+} - \ln\frac{\delta^+}{P^+}\ln\frac{\mu^2}{4m_c^2} - \frac{1}{2}\ln\frac{\mu^2}{m_c^2} \\ &\left. + \ln 2 - 1 - \frac{7\pi^2}{24}\right]. \end{aligned} \tag{46}$$

The contributions of diagrams Fig. 3(a,b) were calculated in ref. [18] at NLO (do not depend on the rapidity regulator introduced in this work). Thus, the sum of all virtual contributions to the gluon TMDFF at NLO is

$$\begin{aligned} &d^{a,b,c,d,e}(z, \mathbf{b}_\perp) \\ &= d^{LO}(z, \mathbf{b}_\perp)\frac{\alpha_s C_A}{2\pi}\left[\frac{1}{\epsilon_{UV}}\left(\frac{\beta_0}{2C_A} + \ln\frac{\delta^{+2}}{P^{+2}}\right) - \frac{1}{\epsilon_{IR}}\right. \\ &+ 2\ln^2\frac{\delta^+}{P^+} + 2\ln\frac{\delta^+}{P^+}\ln\frac{\mu^2}{4m_c^2} + \ln\frac{\mu^2}{m_c^2} \\ &\left. - 4\ln^2 2 + \frac{10}{3}\ln 2 + 2 - \pi^2 + \frac{123 - 10n_f}{27}\right], \end{aligned} \tag{47}$$

where $\beta_0 = 11C_A/3 - 2n_f/3$ and n_f is the number of light quark flavors.

In the δ-regularization scheme, the subtractions related with $\mathbf{Z_b}$ are equal to the soft function [19]. Therefore, the rapidity renormalization factor, defined in (8), becomes

$$R_g(\zeta, \mu) = \frac{1}{\sqrt{S(\mathbf{b}_\perp;\zeta)}}. \tag{48}$$

The virtual contribution of the soft function (9), at one-loop, was computed in ref. [20] and the result is

$$\begin{aligned} S_v = \frac{\alpha_s C_A}{2\pi}&\left[\frac{-2}{\epsilon^2_{UV}} + \frac{2}{\epsilon_{UV}}\ln\frac{\delta^{+2}\zeta}{(P^+)^2\mu^2}\right. \\ &\left. - \ln^2\frac{(\delta^+)^2}{\mu^2} - \frac{\pi^2}{2}\right]. \end{aligned} \tag{49}$$

Therefore, to obtain the pure collinear matrix element, we expand the renormalized TMDFF with the factor $R_g = 1/\sqrt{S_v}$ at first order in α_s, and we obtain

$$d_n = d_n^{(0)} + d_n^{(1)} - \frac{1}{2} d_n^{(0)} S_v = d_n^{(0)} \left(1 + \frac{d_n^{(1)}}{d_n^{(0)}} - \frac{S_v}{2} \right), \tag{50}$$

where $d_n^{(m)}$ is the TMDFF of order m with $m = 0$ meaning LO and $m = 1$ meaning NLO.

The last step is to combine the result (47) with (49) as indicated in (50):

$$\frac{R_g d^{a,b,c,d,e}(z, \mathbf{b}_\perp)}{d^{LO}(z, \mathbf{b}_\perp)} = \frac{\alpha_s C_A}{2\pi} \times \left[\frac{1}{\epsilon_{UV}^2} + \frac{1}{\epsilon_{UV}} \left(\frac{\beta_0}{2C_A} + \ln \frac{\mu^2}{\zeta} \right) - \frac{1}{\epsilon_{IR}} + \frac{1}{2} \ln^2 \frac{\delta^{+2}}{\mu^2} + 2 \ln^2 \frac{\delta^+}{P^+} + 2 \ln \frac{\delta^+}{P^+} \ln \frac{\mu^2}{4m_c^2} + \ln \frac{\mu^2}{m_c^2} - \frac{3\pi^2}{4} - 4 \ln^2 2 + \frac{10}{3} \ln 2 + 2 + \frac{123 - 10 n_f}{27} \right]. \tag{51}$$

Notice that the terms with mixed divergences, $\frac{\ln \delta^+}{\epsilon_{UV}}$, disappeared from the final result because we have renormalized the TMDFF with the factor (48). Moreover, the factor of the single UV pole turns out to be the expected one, which gives the QCD evolution of the gluon TMD operator, and thus appears in all (un)polarized gluon TMDPDFs and TMDFFs (see e.g. ref. [19] for the unpolarized gluon TMDPDF). Therefore, this represents a non-trivial check of the correctness of the calculation, in which we have correctly canceled the rapidity divergences.

VII. CONCLUSION

In this work we have introduced for the first time and studied the gluon transverse-momentum-dependent fragmentation function (TMDFF) into J/ψ, which is the main object of one of the relevant productions mechanisms of the J/ψ at small transverse momentum. We have used non-relativistic QCD (NRQCD) factorization to write the TMDFF as a sum of products of short-distance matching coefficients and long-distance matrix elements (LDMEs).

We have performed an original perturbative calculation of the gluon TMDFF into J/ψ at leading-order and partially at next-to-leading order (only virtual-gluon contributions). After matching the results onto NRQCD we have obtained that the color and angular momentum configuration in which the heavy-quark pair is found at this order is $n = {}^3S_1^{[8]}$. We have also explicitly checked at NLO, by using the δ-regularization scheme, that the rapidity divergences cancel, as expected.

Finally, for the future work we plan to compute the real-gluon contributions at NLO, thus completing the calculation of the TMDFF at that order. This will allow us to perform accurate phenomenological studies to quantitatively asses the relevance of the gluon fragmentation channel to the production of J/ψ at small transverse-momentum.

VIII. INTEGRALS

In this section we illustrate the technique for performing integrals using the δ-regulator. We only show the imaginary part of the result, according to (36) and (42).

The first is as follows

$$I_{ABC} = \int \frac{d^D k}{(2\pi)^D} \frac{1}{[k^2 + i\epsilon][(k - P)^2 + i\epsilon][(P - k) \cdot n + i\epsilon]}, \tag{52}$$

we can do a shift such as $k \to k + P$,

$$I \to I = -\int \frac{d^D k}{(2\pi)^D} \frac{1}{[(k + P)^2 + i\epsilon][k^2 + i\epsilon][k^+ - i\delta^+]}. \tag{53}$$

The fact that the δ-regulator appears in the denominator instead of $+i\epsilon$ is a consequence of (15). The poles in k^- are

$$k_1^- = -\frac{k_\perp^2 + i\epsilon}{k^+}, \qquad k_2^- = -\frac{k_\perp^2 + 4m_c^2 + k^+ P^- + i\epsilon}{k^+ + P^+}. \tag{54}$$

When $k^+ > 0$, $P^+ > 0$, both poles lie in the lower complex half-plane and we can close the contour through the upper half-plane, giving 0 for the integral. When $k^+ < -P^+$, $P^+ > 0$, we are in the same case but in the upper complex half-plane so the result is zero too. However, when $-P^+ < k^+ < 0$, $P^+ > 0$ we find one pole in the lower complex half-plane and one pole in the upper complex half-plane, we choose to close the contour trough the upper half-plane picking the pole k_1^-.

It is convenient to change the integration measure to integrate over k^+, k^- and $k_\perp$, i.e. $d^D k = \frac{dk^+ dk^-}{2} d^{D-2} k_\perp$.

$$I_{ABC} = -\frac{1}{2} \int \frac{dk^+ d^{D-2} k_\perp}{(2\pi)^D [k^+ - i\delta^+]} \times \int_{-\infty}^{\infty} \frac{dk^-}{[(k + P)^2 + i\epsilon][k^2 + i\epsilon]}. \tag{55}$$

Now we integrate in k^- using residues theorem

$$\int_{-\infty}^{\infty} \frac{dk^-}{[(k + P)^2 + i\epsilon][k^2 + i\epsilon]} \tag{56}$$

$$= \frac{2\pi i}{k_\perp^2 P^+ - k^+(k^+ P^- + 4m_c^2)}. \tag{57}$$

Setting $k^+ = zP^+$, to simplify the calculation,

$$I_{ABC} = -\frac{i\pi}{4\pi} \int_{-1}^{0} \frac{dz}{zP^+ - i\delta^+} \times \int \frac{d^{D-2} k_\perp}{(2\pi)^{D-2}} \frac{1}{k_\perp^2 - 4m_c^2 (z^2 + z)}. \tag{58}$$

In this way, we can integrate over $k_\perp$ using the following relation, where $d = 4 - 2\epsilon$, $\delta(>0) \sim 0$,

$$\int \frac{d^{D-2}k_\perp}{(2\pi)^{D-2}} \frac{1}{[k_\perp^2 + \Delta]^{1+\delta}} = \frac{1}{(4\pi)^{1-\epsilon}} \frac{\Gamma(\epsilon+\delta)}{\Gamma(1+\delta)} \Delta^{-\epsilon-\delta}. \tag{59}$$

Given this, we get the following expression for the integral

$$I_{ABC} = \frac{-i}{16\pi^2 P^+} \left(\frac{\pi^2 e^{i\pi}}{m_c^2}\right)^\epsilon \Gamma(\epsilon) \int_{-1}^{0} \frac{dz}{(z-id)(z^2+z)^\epsilon}, \tag{60}$$

with $d = \delta^+/P^+$. The next step is to expand around $\epsilon = 0$ and then, compute the integral in z. Finally, we need to perform the limit $\delta^+ \to 0$ to restore the gauge transformation properties.

$$I_{ABC} = \frac{-i}{16\pi^2 P^+} \left(\frac{\pi e^{i\pi}}{m_c^2}\right)^\epsilon \left[\frac{1}{\epsilon} \ln \frac{\delta^+}{P^+} - \gamma_E \ln \frac{\delta^+}{P^+} + \frac{7\pi^2}{24} - \frac{1}{2} \ln^2 \frac{\delta^+}{P^+}\right]. \tag{61}$$

Another integral we need to calculate is

$$I_{ACD} = \int \frac{d^D k}{(2\pi)^D} \frac{1}{[k^2 + i\epsilon][(P-k)\cdot n + i\epsilon]} \times \frac{1}{[(k-P/2)^2 - m_c^2 + i\epsilon]}. \tag{62}$$

We do the shift $k \to k + P$:

$$I_{ACD} = -\int \frac{d^D k}{(2\pi)^D} \frac{1}{[(k+P)^2 + i\epsilon][k^+ - i\delta^+]} \times \frac{1}{[(k+P/2)^2 - m_c^2 + i\epsilon]}. \tag{63}$$

In this case, the k^- poles are

$$k_1^- = -\frac{k_\perp^2 + 4m_c^2 + k^+P^+ + i\epsilon}{k^+ + P^+}, \tag{64}$$

$$k_2^- = -\frac{k_\perp^2 + k^+P^-/2 + i\epsilon}{k^+ + P^+/2}. \tag{65}$$

Then, the integral is not zero only when $-P^+ < k^+ < -P^+/2$, $P^+ > 0$. We have the same expression as in (55) but now the result of doing the k^- integral using the residue theorem is

$$\int_{-\infty}^{\infty} \frac{dk^-}{[(k+P)^2 + i\epsilon][(k+P/2)^2 - m_c^2 + i\epsilon]} = \tag{66}$$

$$-\frac{2}{P^+} \frac{2\pi i}{[k_\perp^2 - (k^+)^2 P^-/P^+ - 4m_c^2(2k^+/P^+ + 1)]}, \tag{67}$$

setting $k^+ = zP^+$,

$$I_{ACD} = \frac{i}{2\pi} \int_{-1}^{-1/2} \frac{dz}{zP^+ - i\delta^+} \times \tag{68}$$

$$\int \frac{d^{D-2}k_\perp}{(2\pi)^{D-2}} \frac{1}{[k_\perp^2 - 4m_c^2(z^2+2z+1)]}, \tag{69}$$

and computing the integral in $k_\perp$ with (59)

$$I = \frac{i}{8\pi P^+} \left(-\frac{\pi}{m_c^2}\right)^\epsilon \Gamma(\epsilon) \int_{-1}^{-1/2} \frac{dz}{z - id} \frac{1}{(z^2+2z+1)^\epsilon}, \tag{70}$$

where $d = \delta^+/P^+$. In the last step we make the expansion in ϵ, then we integrate in z and finally we make the expansion in δ^+:

$$I_{ACD} = \frac{i}{16\pi^2 P^+} \left(\frac{\pi e^{i\pi}}{m_c^2}\right)^\epsilon \left[-\frac{2}{\epsilon} \ln 2 + \gamma_E 2 \ln 2 \right. \tag{71}$$

$$\left. -\frac{1}{3}(\pi^2 + 6\ln^2 2)\right]. \tag{72}$$

The last independent integral we need to perform is

$$I_{BCD} = \int \frac{d^D k}{(2\pi)^D} \frac{1}{[(k-P)^2 + i\epsilon][(P-k)\cdot n + i\epsilon]} \times \frac{1}{[(k-P/2)^2 + i\epsilon]}. \tag{73}$$

We perform the shift $k \to k + P$

$$I_{BCD} = -\int \frac{d^D k}{(2\pi)^D} \frac{1}{[k^2 + i\epsilon][k^+ - i\delta^+]} \times \frac{1}{[(k+P/2)^2 - m_c^2 + i\epsilon]}, \tag{74}$$

and the poles in k^- are

$$k_1^- = -\frac{k_\perp^2 + i\epsilon}{k^+}, \qquad k_2^- = -\frac{k_\perp^2 + k^+P^-/2 + i\epsilon}{k^+ + P^+/2}. \tag{75}$$

Then, we are only interested in region $-P^+/2 < k^+ < 0$. We change the integration measure:

$$I_{BCD} = -\frac{1}{2} \int \frac{dk^+ d^{D-2}k_\perp}{(k^+ - i\delta^+)(2\pi)^D} \times \tag{76}$$

$$\int_{-\infty}^{\infty} \frac{dk^-}{[k^2 + i\epsilon][(k+P/2)^2 - m_c^2 + i\epsilon]}. \tag{77}$$

Performing the integral in k^- by residues method and setting $k^+ = zP^+$

$$I_{BCD} = \frac{i}{2\pi} \int_{-1/2}^{0} \frac{dz}{zP^+ - i\delta^+} \int \frac{d^{D-2}k_\perp}{(2\pi)^{D-2}} \frac{1}{[k_\perp^2 - 4m_c^2 z^2]}. \tag{78}$$

We perform the integral in $k_\perp$ using (59)

$$I_{BCD} = \frac{i}{8\pi^2 P^+} \left(\frac{\pi e^{i\pi}}{m_c^2}\right)^\epsilon \Gamma(\epsilon) \int_{-1/2}^{0} \frac{dz}{(z-id)z^{2\epsilon}}, \tag{79}$$

where $d = \delta^+/P^+$. At the end we expand in ϵ, perform the integral in z and then expand around $\delta^+ = 0$:

$$I_{BCD} = \frac{-i}{16\pi^2 P^+} \left(\frac{\pi e^{i\pi}}{m_c^2}\right)^\epsilon \left[-\frac{2}{\epsilon} \ln \frac{2\delta^+}{P^+} + \gamma_E 2 \ln \frac{2\delta^+}{P^+} + \frac{11}{6}\pi^2 + 2\ln^2 2 - 2\ln^2 \frac{\delta^+}{P^+}\right]. \tag{80}$$

These three integrals that we have performed so far are the only independent integrals involved in the calculation of the short-distance coefficients. However, there are other integrals involved that we can put in function of these three integrals:

$$4m_c^2 I_{ABCD} = I_{ACD} + I_{BCD} - 2I_{ABC} \tag{81}$$

$$4m_c^2 I_{ABD} = 2(I_{AD} - I_{AB}) \tag{82}$$

Their expressions are

$$I_{ABCD} = \frac{i}{4m_c^2 P^+}\left(-\frac{3}{16\pi^2}\ln^2\frac{\delta^+}{P^+} + \frac{1}{4\pi^2}\ln^2 2 + \frac{19}{192}\right), \tag{83}$$

$$I_{ABD} = i\frac{\ln 2}{16\pi^2 m_c^2}. \tag{84}$$

For the most elementary integrals it is not necessary to use the δ-regulator because they do not have rapidity divergences. They are tabulated and at order $\mathcal{O}(\epsilon^0)$ are the following

$$I_{AB} = \frac{i}{16\pi^2}\left[\frac{1}{\epsilon} + \ln\frac{\mu^2}{m_c^2} - \gamma_E + 2 + \ln\pi\right] \tag{85}$$

$$I_{AD} = \frac{i}{16\pi^2}\left[\frac{1}{\epsilon} + \ln\frac{\mu^2}{m_c^2} - \gamma_E + 2 + \ln 4\pi\right] \tag{86}$$

ACKNOWLEDGMENTS

I would like to thank Rafael Fernández del Castillo from UCM for his help and collaboration in this work. I would also like to thank IPARCOS (UCM) for the financial support.

[1] J.-P. Lansberg, New Observables in Inclusive Production of Quarkonia, Phys. Rept. **889**, 1 (2020), arXiv:1903.09185 [hep-ph].

[2] E. Chapon *et al.*, Prospects for quarkonium studies at the high-luminosity LHC, Prog. Part. Nucl. Phys. **122**, 103906 (2022), arXiv:2012.14161 [hep-ph].

[3] S. Acharya *et al.* (ALICE), Inclusive J/ψ production at midrapidity in pp collisions at $\sqrt{s} = 13$ TeV, Eur. Phys. J. C **81**, 1121 (2021), arXiv:2108.01906 [nucl-ex].

[4] B. Aubert *et al.* (BaBar), Measurement of J/ψ production in continuum e^+e^- annihilations near $\sqrt{s} = 10.6$ GeV, Phys. Rev. Lett. **87**, 162002 (2001), arXiv:hep-ex/0106044.

[5] U. D'Alesio, F. Murgia, C. Pisano, and P. Taels, Azimuthal asymmetries in semi-inclusive J/ψ + jet production at an EIC, Phys. Rev. D **100**, 094016 (2019), arXiv:1908.00446 [hep-ph].

[6] M. G. Echevarria, Y. Makris, and I. Scimemi, Quarkonium TMD fragmentation functions in NRQCD, JHEP **10**, 164, arXiv:2007.05547 [hep-ph].

[7] T. Becher, A. Broggio, and A. Ferroglia, *Introduction to Soft-Collinear Effective Theory*, Vol. 896 (Springer, 2015) arXiv:1410.1892 [hep-ph].

[8] C. W. Bauer, D. Pirjol, and I. W. Stewart, Soft collinear factorization in effective field theory, Phys. Rev. D **65**, 054022 (2002), arXiv:hep-ph/0109045.

[9] A. Vladimirov, V. Moos, and I. Scimemi, Transverse momentum dependent operator expansion at next-to-leading power, JHEP **01**, 110, arXiv:2109.09771 [hep-ph].

[10] M. G. Echevarría, A. Idilbi, and I. Scimemi, Soft and Collinear Factorization and Transverse Momentum Dependent Parton Distribution Functions, Phys. Lett. B **726**, 795 (2013), arXiv:1211.1947 [hep-ph].

[11] G. T. Bodwin, E. Braaten, and G. P. Lepage, Rigorous QCD analysis of inclusive annihilation and production of heavy quarkonium, Phys. Rev. D **51**, 1125 (1995), [Erratum: Phys.Rev.D 55, 5853 (1997)], arXiv:hep-ph/9407339.

[12] M. G. Echevarria, I. Scimemi, and A. Vladimirov, Unpolarized Transverse Momentum Dependent Parton Distribution and Fragmentation Functions at next-to-next-to-leading order, JHEP **09**, 004, arXiv:1604.07869 [hep-ph].

[13] A. V. Manohar and I. W. Stewart, The Zero-Bin and Mode Factorization in Quantum Field Theory, Phys. Rev. D **76**, 074002 (2007), arXiv:hep-ph/0605001.

[14] W. J. Waalewijn, *Factorization at the LHC: From PDFs to Initial State Jets*, Other thesis (2010), arXiv:1104.5164 [hep-ph].

[15] E. Braaten and Y.-Q. Chen, Helicity decomposition for inclusive J / psi production, Phys. Rev. D **54**, 3216 (1996), arXiv:hep-ph/9604237.

[16] M. G. Echevarria, I. Scimemi, and A. Vladimirov, Universal transverse momentum dependent soft function at NNLO, Phys. Rev. D **93**, 054004 (2016), arXiv:1511.05590 [hep-ph].

[17] E. Braaten and Y.-Q. Chen, Dimensional regularization in quarkonium calculations, Phys. Rev. D **55**, 2693 (1997), arXiv:hep-ph/9610401.

[18] E. Braaten and J. Lee, Next-to-leading order calculation of the color octet 3S(1) gluon fragmentation function for heavy quarkonium, Nucl. Phys. B **586**, 427 (2000), arXiv:hep-ph/0004228.

[19] M. G. Echevarria, A. Idilbi, and I. Scimemi, On Rapidity Divergences in the Soft and Collinear Limits of QCD, Int. J. Mod. Phys. Conf. Ser. **25**, 1460005 (2014), arXiv:1310.8541 [hep-ph].

[20] M. G. Echevarria, T. Kasemets, P. J. Mulders, and C. Pisano, QCD evolution of (un)polarized gluon TMD-PDFs and the Higgs q_T-distribution, JHEP **07**, 158, [Erratum: JHEP 05, 073 (2017)], arXiv:1502.05354 [hep-ph].